Wideband Microwave Phase Noise Analyzer Based on All-Optical Microwave Signal Processing

Yifeng Xie, Pei Zhou, *Member, IEEE*, Zhidong Jiang, Zhihua Zhou, and Nianqiang Li, *Member, IEEE*

***Abstract*—An approach for wideband phase noise measurement of microwave signal sources is proposed based on all-optical microwave signal processing. In the proposed scheme, an optical carrier is sequentially modulated by the signal under test (SUT) in a phase modulator and a dual-polarization modulator to generate two +1st-order sidebands with orthogonal polarizations. A time delay is introduced between two sidebands by a span of low-loss optical fiber. Combined with a polarization controller and a polarizer, photonic microwave downconversion with a desired phase shift and time delay can be realized after photodetection, and the phase noise of the SUT can be calculated thereafter. Since all the microwave signal processing functions in the conventional photonic-delay-line-based phase noise measurement system are implemented in the optical domain, the proposed scheme has a large operational bandwidth and a high measurement sensitivity. In the experimental demonstration, accurate phase noise measurement of SUTs is achieved in a frequency range of 10-35 GHz, and a phase noise floor as low as −132.16 dBc/Hz at 10 kHz is obtained.**

***Index Terms*—All-optical microwave signal processing, frequency discriminator, microwave photonics, phase noise.**

I. Introduction

PHASE noise, which denotes the short-term frequency stability of a microwave signal, is an important parameter to evaluate the performance of a microwave signal source [1]–[4]. Due to the rapid development of ultralow phase noise microwave signal sources [5], [6] and their wide applications in radar, communication and navigation systems [7]–[9], highly accurate phase noise measurement is now of great importance. In recent years, the photonic-delay-line-based frequency discriminator method, which achieves high measurement sensitivity with the assistance of a low-loss optical fiber, has attracted much attention [10], [11]. Consequently, great efforts have been made to improve its overall performance. For instance, optical frequency comb and carrier suppression interferometer techniques have been introduced to enhance the measurement sensitivity [12]–[14]. To eliminate the calibration procedure, quadrature phase demodulation based on in-phase and quadrate (I/Q) mixing and digital signal processing is adopted [13], [15]–[17]. Recently, multiple functions, such as microwave signal generation and frequency measurement, have also been integrated into the original phase noise measurement system [18]–[20]. However, among the previously reported photonic-delay-line-based phase noise measurement systems, the operational bandwidth is usually restricted by electrical devices (e.g., electrical mixers, phase shifters and amplifiers). To cope with this problem, the functions of microwave phase shifting [21], [22] or frequency mixing [23] are realized based on microwave photonic technologies to achieve bandwidth enhancement. Nevertheless, an all-optical phase noise measurement system that realizes all microwave signal processing functions in the optical domain, has rarely been reported [24]. In [24], an electro-optical polarization modulator (PolM) is used to realize the function of phase shifting. However, owing to its limited application scenarios [25], [26], the customized PolM not only makes the system costly, but also limits the operational bandwidth to be further expanded [27].

In this paper, a wideband phase noise analyzer based on all-optical microwave signal processing is demonstrated theoretically and experimentally. In the proposed scheme, an optical carrier is sequentially modulated by the signal under test (SUT) in a phase modulator (PM) and a dual-polarization Mach-Zehnder modulator (Dpol-MZM) to generate two +1st-order sidebands with orthogonal polarizations. A time delay is introduced between two sidebands by a section of low-loss optical fiber. Combined with a polarization controller (PC) and a polarizer (Pol), photonic microwave downconversion with tunable phase shift can be realized after photodetection, and the phase noise of the SUT can be calculated thereafter. In the experiment, a microwave photonic downconverter with phase shifting ability is first demonstrated. Afterwards, accurate phase noise measurement of SUTs is achieved in a frequency range of 10-35 GHz, and a phase noise floor as low as −132.16 dBc/Hz at 10 kHz is obtained. The proposed scheme features compactness, high sensitivity and a wide measurement range, which can find applications in the evaluation of wideband tunable microwave signal sources with very low phase noise.

Manuscript received April 29, 2022; revised June 6, 2022; accepted June 16, 2022. Date of publication June 20, 2022; date of current version July 8, 2022. This work was supported in part by the National Natural Science Foundation of China under Grants 62001317, 62171305, and 62004135, in part by the Natural Science Foundation Program of Jiangsu Province under Grant BK20200855, in part by the Natural Science Research Project of Jiangsu Higher Education Institutions of China under Grants 20KJB510011 and 20KJA416001, and in part by the National Undergraduate Training Program for Innovation and Entrepreneurship under Grant 202010285044. *(Corresponding author: Pei Zhou.)*

The authors are with the School of Optoelectronic Science and Engineering, Soochow University, Suzhou 215006, China, and also with the Key Lab of Advanced Optical Manufacturing Technologies of Jiangsu Province & Key Lab of Modern Optical Technologies of Education Ministry of China, Soochow University, Suzhou 215006, China (e-mail: oreoxyf@outlook.com; peizhou@suda.edu.cn; 20205239013@stu.suda.edu.cn; zhouzhihua2022@163.com; nli@suda.edu.cn).

Digital Object Identifier 10.1109/JPHOT.2022.3184596

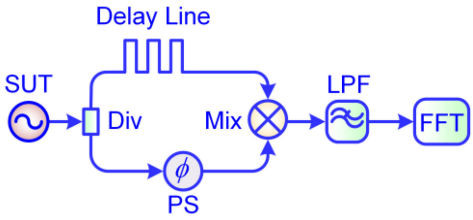

Fig. 1. Schematic diagram of the typical delay-line-based frequency discriminator method. SUT: Signal under test; Div: Electrical power divider; PS: Microwave phase shifter; Mix: Microwave mixer; LPF: Low pass filter; FFT: Fast Fourier transform.

II. Principle

A. Typical Delay-Line-based Frequency Discriminator Method

For a better understanding of the proposed phase noise measurement system, the typical delay-line-based frequency discriminator method is briefly introduced, as shown in Fig. 1 [3]. Mathematically, the SUT can be expressed as

$$S(t) = V_0 \cos[\omega_0 t + \varphi(t)] \tag{1}$$

where V_0 and ω_0 are the amplitude and angular frequency of the signal, respectively, and φ(t) is the phase fluctuation. Then, it is divided into two branches by an electrical power divider (Div). In the upper branch, a proper time delay of τ is introduced by a section of electrical cables, and the delayed signal is given by

$$V_1(t) = \frac{\sqrt{2}}{2} V_0 \cos[\omega_0 (t-\tau) + \varphi(t-\tau)] \tag{2}$$

In the lower branch, the microwave signal passes through a microwave phase shifter (PS) to obtain a tunable phase shift of θ before mixing with the upper-branch signal. The phase-shifted signal before the microwave mixer (Mix) is

$$V_2(t) = \frac{\sqrt{2}}{2} V_0 \cos[\omega_0 t + \varphi(t) + \theta] \tag{3}$$

Subsequently, the electrical signals in both branches are mixed with each other before being sent to a low pass filter (LPF). The voltage signal at the output of the LPF is

$$V_O(t) \propto \cos[\varphi(t) - \varphi(t-\tau) + \omega_0 \tau + \theta] \tag{4}$$

By tuning the PS, the phase difference between the two signals in both branches can be adjusted in quadrature, i.e., $\omega_0\tau + \theta = 2k\pi + \pi/2$ is satisfied, where k is an integer. Therefore, the voltage signal becomes

$$V_O(t) \propto \sin[\varphi(t) - \varphi(t-\tau)] \approx [\varphi(t) - \varphi(t-\tau)] \tag{5}$$

Based on (5), the power spectral density (PSD) of $V_O(t)$ can be represented as

$$S_O(f) \propto \sin^2(\pi f \tau) S_\varphi(f) \tag{6}$$

where $S_\varphi(f)$ is the PSD of the phase fluctuation and $S_O(f)$ can be measured by a fast Fourier transform (FFT) analyzer. Therefore, the single sideband (SSB) phase noise power spectrum, denoted as $L(f)$, can be obtained as

$$L(f) = \frac{S_\varphi(f)}{2} \propto \frac{S_O(f)}{\sin^2(\pi f \tau)} \tag{7}$$

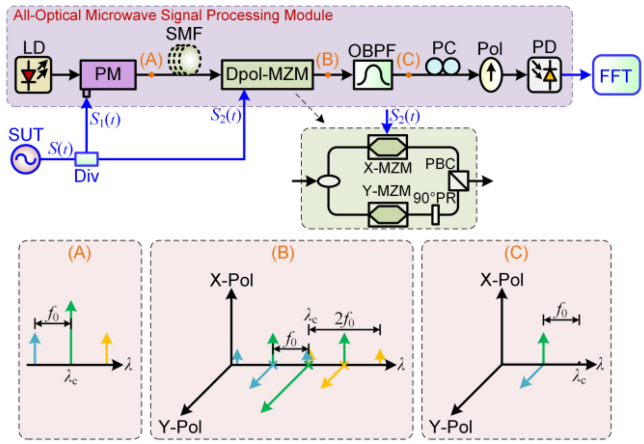

Fig. 2. Schematic diagram of the proposed all-optical phase noise measurement method. LD: Laser diode; PM: Phase modulator; SMF: Single mode fiber; Dpol-MZM: Dual-polarization Mach-Zehnder modulator; PR: Polarization rotator; PBC: Polarization beam combiner; OBPF: Optical bandpass filter; PC: Polarization controller; Pol: Polarizer; PD: Photodetector.

B. Proposed All-Optical Phase Noise Measurement Method

Fig. 2 provides the schematic diagram of the proposed all-optical phase noise measurement method. The purple dashed box is an all-optical microwave signal processing module, which consists of a laser diode (LD), a PM, a section of single mode fiber (SMF), a Dpol-MZM, an optical bandpass filter (OBPF), a PC, a Pol, and a photodetector (PD). An optical carrier from the LD is sequentially modulated by the SUT in a PM and a Dpol-MZM to generate two +1st-order sidebands with orthogonal polarizations. A time delay is introduced between two sidebands by a section of SMF. After the Dpol-MZM, an OBPF is applied to select two orthogonally polarized +1st-order sidebands with different time delays. Combined with the PC and the Pol, photonic microwave downconversion with a desired phase shift can be achieved after photodetection. Finally, the output signal from the PD is sent to an FFT analyzer for phase noise calculation. Compared with the phase noise measurement system in Fig. 1, neither a microwave mixer nor a microwave phase shifter is needed. The functions of microwave mixing and microwave phase shifting in the system are achieved in the optical domain by the all-optical microwave signal processing module, namely, a microwave photonic downconverter with phase shifting ability is realized. Its principle and the corresponding all-optical phase noise measurement system are theoretically analyzed as follows.

1) Microwave Photonic Downconverter With Phase Shifting Ability: Assuming that the PM is driven by a local oscillator (LO) signal $S_1(t)$, whose amplitude and angular frequency are V_1 and ω_{LO}, respectively, the optical signal at the output of the PM is written as

$$E_1(t) = E_0 \exp[j\omega_c t + j\beta_1 \cos \omega_{LO} t] \tag{8}$$

In (8), E_0 and ω_c are the amplitude and angular frequency of the optical carrier, respectively, and $\beta_1 = \pi V_1 / V_{\pi 1}$ is the phase modulation index, with $V_{\pi 1}$ being the half-wave voltage of the PM. Then, the optical signal from the PM is sent to the Dpol-MZM. The structure of the Dpol-MZM is depicted in the green dashed box in Fig. 2, which consists of two parallel sub-MZMs (X-MZM and Y-MZM), a 90° polarization rotator (PR) and a polarization beam combiner (PBC). In the modulator, the X-MZM driven by a radio frequency (RF) signal $S_2(t)$ with an amplitude of V_2 and angular frequency at ω_{RF} is biased at the minimum transmission point (MITP) for carrier-suppressed double-sideband (CS-DSB) modulation, and no modulation signal is applied to the Y-MZM. In this case, at the output of the Dpol-MZM, the optical fields in two orthogonal polarization states, i.e., *x* polarization and *y* polarization, are

$$\begin{bmatrix} E_{X1}(t) \\ E_{Y1}(t) \end{bmatrix} = \frac{\sqrt{2}}{2} E_1(t) \cdot \begin{bmatrix} \exp(j\beta_2 \cos \omega_{RF} t + j\pi/2) + \exp(-j\beta_2 \cos \omega_{RF} t - j\pi/2) \\ 1 \end{bmatrix} \tag{9}$$

where $\beta_2 = \pi V_2 / V_{\pi 2}$ is the modulation index and $V_{\pi 2}$ is the half-wave voltage of the X-MZM. After the Dpol-MZM, an OBPF is applied to select two $+1^{st}$-order optical modulation sidebands in both polarizations. Based on the Jacobi-Anger expansion, the optical signal after the OBPF can be expressed as

$$\begin{bmatrix} E_{X2}(t) \\ E_{Y2}(t) \end{bmatrix} = \frac{\sqrt{2}}{2} E_0 \exp(j\omega_c t) \begin{bmatrix} -2J_0(\beta_1) J_1(\beta_2) \exp(j\omega_{RF} t) \\ jJ_1(\beta_1) \exp(j\omega_{LO} t) \end{bmatrix} \tag{10}$$

where $J_n(\cdot)$ is the n^{th}-order Bessel function of the first kind. Next, a Pol is used to align the two orthogonal signals in (10) into the same polarization direction. The optical signal after the Pol is

$$E_2(t) = \cos\alpha \cdot E_{X2} + \sin\alpha \cdot E_{Y2} \tag{11}$$

where α is the angle of the principal axes between the Dpol-MZM and the Pol, and can be adjusted by tuning the PC before the Pol. After photodetection by the PD, the downconverted signal can be extracted, and the photocurrent can be approximately expressed as

$$I_{PD}(t) \propto \sin[(\omega_{RF} - \omega_{LO})t + 2\alpha] \tag{12}$$

As can be seen from (12), the RF frequency ω_{RF} is downconverted to an intermediate frequency (IF) of $\omega_{IF} = \omega_{RF} - \omega_{LO}$. More importantly, the phase of the IF signal can be continuously tuned in a full 360° range by adjusting the PC before the Pol. In addition, the amplitude of the IF signal will not change during the phase shifting.

2) Wideband Phase Noise Measurement: As shown in Fig. 2, an all-optical phase noise measurement system is built based on the aforementioned microwave photonic downconverter with phase shifting ability. The schematic optical spectra at some key nodes are also illustrated in the dashed boxes in the lower part of Fig. 2. In the system, $S_1(t)$ and $S_2(t)$ are two identical signals from the SUT to serve as drive signals of the PM and Dpol-MZM, respectively. The expression of the SUT is given in (1). Besides, a proper time delay of τ is introduced by a section of SMF between the PM and Dpol-MZM. The optical signal after the OBPF can be rewritten as

$$\begin{bmatrix} E_{X2}(t) \\ E_{Y2}(t) \end{bmatrix} = \frac{\sqrt{2}}{2} E_0 \exp[j\omega_c (t-\tau)] \cdot \begin{bmatrix} -2J_0(\beta_1) J_1(\beta_2) \exp[j\omega_0 t + j\varphi(t)] \\ jJ_1(\beta_1) \exp[j\omega_0 (t-\tau) + j\varphi(t-\tau)] \end{bmatrix} \tag{13}$$

In (12), the output current from the PD now becomes

$$I_{PD}(t) \propto \sin[\varphi(t) - \varphi(t-\tau) + \omega_0 \tau + 2\alpha] \tag{14}$$

By tuning the PC, α can be adjusted to satisfy $\omega_0 \tau + 2\alpha = 2k\pi$, where *k* is an integer, and (14) can be simplified to

$$I_{PD}(t) \propto \sin[\varphi(t) - \varphi(t-\tau)] \approx [\varphi(t) - \varphi(t-\tau)] \tag{15}$$

It can be seen that (15) is the same as (5), and the SSB phase noise power spectrum $L(f)$ can be calculated in the same way thereafter. Since all the microwave signal processing functions in the conventional delay-line-based frequency discriminator method are implemented in the optical domain, the proposed phase noise measurement scheme has a large operational bandwidth and a high measurement sensitivity.

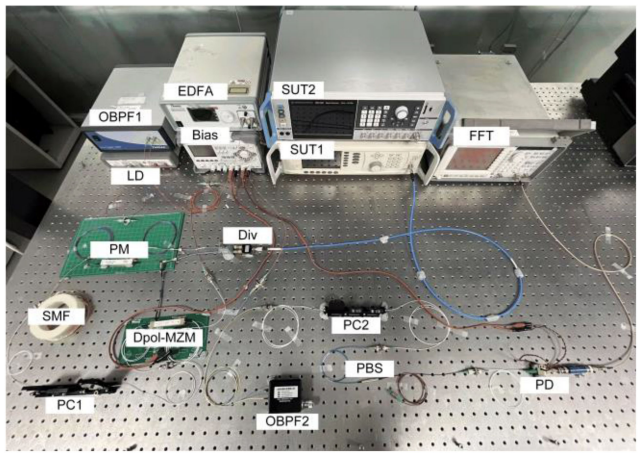

Fig. 3. Photograph of the experimental setup.

III. Experimental Results and Discussion

A. Microwave Photonic Downconverter With Phase Shifting Ability

To verify the feasibility of the proposed system, a proof-of-concept experiment is carried out according to the setup shown in Fig. 2. First, an experiment is performed to verify the feasibility of the microwave photonic downconverter with phase shifting ability. A photograph of the experimental setup is shown in Fig. 3. In the experiment, an optical carrier at 1550.116 nm from the LD (Agilent N7714A) with a maximum power of 16 dBm is sent to a 40-GHz PM (iXblue MPZ-LN-40). The Dpol-MZM (Fujitsu FTM7980EDA) has a 3-dB bandwidth of 22 GHz and a half-wave voltage of 1.8 V. The RF and LO signals are generated from two microwave signal sources (R&S SMA100B;

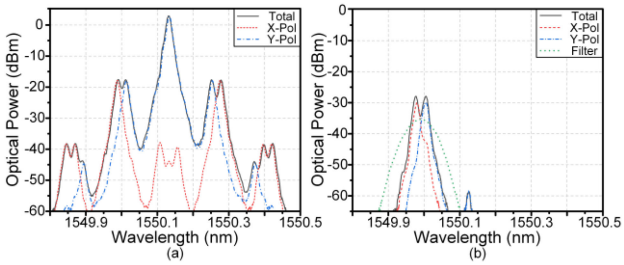

Fig. 4. (a) Optical spectra after the Dpol-MZM (black) and its spectral components in the *x* polarization (red) and *y* polarization (blue); (b) Optical spectra after the OBPF (black), its spectral components in the *x* polarization (red) and *y* polarization (blue) and the transmission response of the OBPF (green).

Anritsu MG3692B). After the Dpol-MZM, an OBPF (Finisar Waveshaper 1000A) with a roll-off factor of 400 dB/nm is used to extract a pair of $+1^{st}$-order sidebands. An erbium-doped fiber amplifier (EDFA, Amonics AEDFA-PA-35-B-FA) and another OBPF (WL Photonics Inc.) with a bandwidth of 0.78 nm are applied to boost the optical power of the extracted sidebands and suppress the amplified spontaneous emission (ASE) noise of EDFA, respectively. Both devices can be saved if an LD with a higher output power, and/or a Dpol-MZM with a smaller insertion loss is available. Subsequently, the obtained signal transmits through the PC and a Pol before being detected by a 20-GHz PD (Optilab PD-20). The output electrical signal from the PD is measured in a 20-GHz oscilloscope (LeCroy WaveMaster 820Zi-B). Here, a polarization beam splitter (PBS) with a polarization extinction ratio of over 30 dB serves as a Pol. The optical spectra are monitored by an optical spectrum analyzer (Ando AQ6317B), while the electrical spectra are measured by an electrical signal analyzer (R&S FSV40).

The frequency downconversion performance is investigated by applying an 18-GHz RF signal and a 15-GHz LO signal to the system. The output power of the RF and LO signals are 15.2 dBm and 13 dBm, respectively. The optical spectra after the Dpol-MZM and after the OBPF as well as the transmission response of the optical filter are plotted in Fig. 4. As shown in Fig. 4(a), the optical signal in the Y-MZM is not modulated, whereas it is modulated by an 18-GHz RF signal and carrier-suppressed by 47 dB at the X-MZM. As shown in Fig. 4(b), a pair of orthogonally polarized +1st-order sidebands are selected after the OBPF, and other optical components are significantly suppressed. Fig. 5(a) is the electrical spectrum of the IF with a frequency of 3 GHz, which is measured after the PD. No additional low-pass electrical filter after PD is needed to remove unwanted signals, and no obvious spur components are observed. Fig. 5(b) shows the normalized temporal waveforms of the 3-GHz IF signal with different phase shifts. In Fig. 5(b), by adjusting the PC, the downconverted signal with phase shifts of 0° (360°), 90°, 180°, and 270° are captured. In addition, the amplitude of the waveform with different phase shifts remains almost unchanged, which agrees well with the theoretical analysis. Without loss of generality, the LO frequency is adjusted to 16 GHz, and the results of the 2-GHz IF signal are shown in Fig. 5(c) and 5(d). The results confirm that photonic microwave downconversion with tunable phase shift is successfully realized.

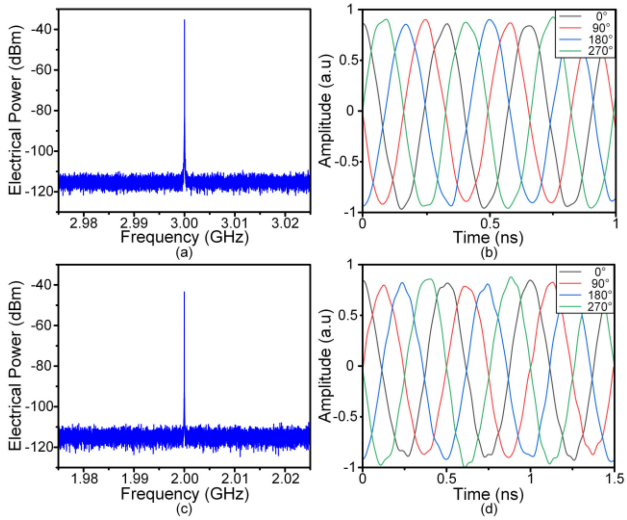

Fig. 5. Electrical spectra of the (a) 3-GHz and (c) 2-GHz IF signals; temporal waveforms of the (b) 3-GHz and (d) 2-GHz IF signals with a phase step of 90°.

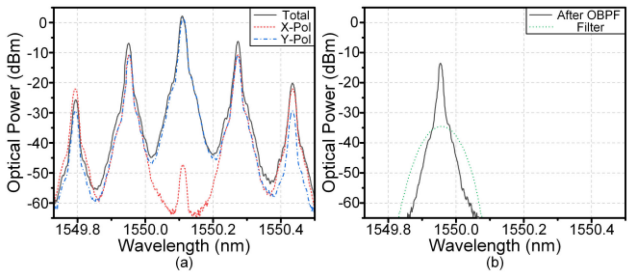

Fig. 6. (a) Optical spectra after the Dpol-MZM (black) and its spectral components in the *x* polarization (red) and *y* polarization (blue); (b) Optical spectra after the OBPF (black) and the transmission response of the OBPF (green).

B. Wideband Phase Noise Measurement

Next, we carried out a wideband phase noise measurement experiment. It is worth noting that during the phase noise measurement, the electrical signal after PD is a baseband signal, and a low-speed PD with MHz bandwidth would be sufficient. In the experiment, a 20-GHz signal from Anritsu MG3692B is used as the SUT, and the length of the SMF is 2 km. As a comparison, the optical spectra after the Dpol-MZM and OBPF as well as its transmission response are shown in Fig. 6(a) and 6(b). In Fig. 6(a), a carrier suppression ratio of approximately 50 dB is observed in the X-Pol of the Dpol-MZM. As shown in Fig. 6(b), spectrally pure $+1^{st}$-order optical sidebands are obtained.

Before the phase noise calculation at an FFT analyzer (Agilent 35670A), it is vital that the PC should be tuned to adjust the phase shift between $S_1(t)$ and $S_2(t)$, and $\omega_0\tau + 2\alpha = 2k\pi$ is satisfied. Then, the phase noise of the 20-GHz signal is tested, and the result is plotted in Fig. 7(a). As a validation of the obtained phase noise, the phase noise result measured by a commercial signal analyzer (R&S FSV40) is also included. It can be found that the two curves agree well with each other when the offset frequency is over 1 kHz, which proves the measurement accuracy of the established system. The deviation of close-in phase noise with a

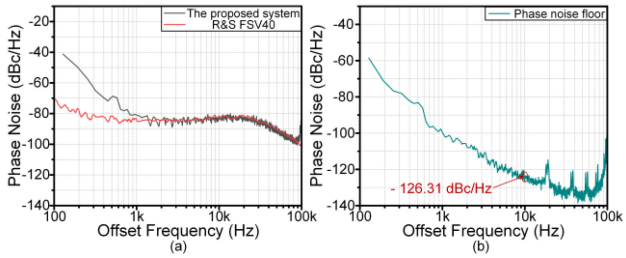

Fig. 7. (a) Phase noise of a 20-GHz microwave signal measured by the proposed system (black), and that measured by a commercial signal analyzer R&S FSV40 (red); (b) Phase noise floor of the established system using a 2-km SMF.

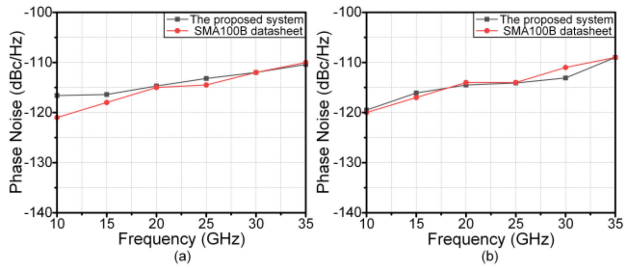

Fig. 8. Phase noise at offset frequencies of (a) 10 kHz and (b) 20 kHz of a wideband signal source (R&S SMA100B) measured by the proposed system (black) and those provided by the datasheet (red).

slope of $1/f$ is mainly due to the flicker noise in the PD. By using a high-linear PD with better noise performance, it can be greatly reduced [28]. Then, the phase noise floor of the established system, which indicates its measurement sensitivity, is evaluated by replacing the 2-km SMF with an optical attenuator that has the same insertion loss [14]. As shown in Fig. 7(b), a low noise floor of −126.31 dBc/Hz at a 10 kHz offset is achieved, which means that good sensitivity is achieved by the proposed method. In Fig. 7(b), some spurs at integral multiples of 18 kHz are observed, which may be induced by the internal noise of the FFT analyzer, since they still exist when no input signal is applied.

In addition to the good performance in measurement accuracy and sensitivity, another advantage of the proposed phase noise measurement system is the large measurement frequency range because of the realization of all optical microwave signal processing. To demonstrate the wideband tunability of the proposed system, the frequency of the microwave signal generated from a wideband microwave signal source (R&S SMA100B) is adjusted from 10 to 35 GHz with a step of 5 GHz. The measured phase noise at 10 kHz and 20 kHz offsets is shown in Fig. 8(a) and 8(b), where typical values provided by the datasheet are also included [29]. It can be seen that the measured results fit quite well with those in the datasheet. The difference is kept within 2 dB, except for the 4.4-dB difference at a 10 kHz offset at 10 GHz. The relatively large deviation at 10 GHz is induced by the residual optical carrier component, which is not fully suppressed by the OBPF. This result proves that the proposed system is able to operate from 10 to 35 GHz with outstanding measurement accuracy. In the experiment, the minimum operational frequency is restricted by the roll-off factor of the OBPF,

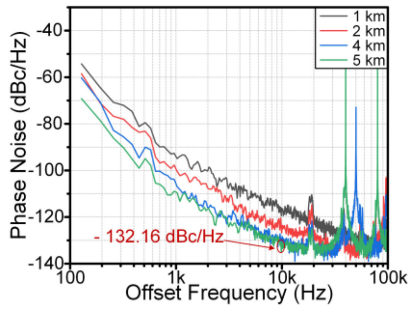

Fig. 9. Phase noise floor of the proposed system with different lengths of SMF.

and the upper limit of the operational frequency is attributed to the 3-dB bandwidth of the Dpol-MZM. On the one hand, the minimum operational frequency can be further expanded to 3.7 GHz if a 1500 dB/nm roll-off factor optical filter is used [30], or cascading a dual-drive Mach-Zehnder modulator and a dual-polarization dual-parallel Mach-Zehnder modulator with two electrical 90-degree hybrids to avoid the use of an OBPF. On the other hand, by using a Dpol-MZM with a larger 3-dB bandwidth, e.g., 110 GHz [31], the upper limit of the operational frequency also has the potential to be greatly expanded.

Finally, the phase noise floor of the proposed system when using different lengths of fiber is investigated in Fig. 9. From Fig. 9, one can conclude that the sensitivity of the system is improved with increasing fiber length. However, the reliable range of offset frequency is sacrificed. Specifically, the measured phase noise floor reaches −132.16 dBc/Hz at a 10 kHz offset for the 5-km fiber. It should be noted that this result can be further improved if the use of an EDFA and a second OBPF is avoided [32] by using an LD with a higher output power and/or a Dpol-MZM with a smaller insertion loss [31]. Besides, if a low-speed PD with a bandwidth of several MHz and possibly higher sensitivity is applied, the measurement sensitivity is also expected to be improved. In addition, the phase noise measurement sensitivity can be further enhanced by building two identical systems to implement two-channel cross-correlation, and an improvement of approximately 15 dB can be realized by averaging 1000 times [33], [34].

IV. Conclusion

In conclusion, we have proposed and demonstrated a novel scheme for wideband phase noise measurement based on all-optical microwave signal processing. Since all the microwave signal processing functions in the conventional delay-line-based phase noise measurement system are implemented in the optical domain, e.g., microwave frequency mixing and phase shifting, the proposed scheme can achieve both a large operational bandwidth and a high measurement sensitivity. The key unit of the proposed method is the all-optical microwave signal processing module, and photonic microwave downconversion with a tunable phase shift over the 360° range is successfully obtained. Based on the microwave photonic downconverter with phase shifting ability, the phase noise of microwave signals is experimentally measured. Accurate phase noise measurement

of SUTs is achieved in a wide frequency range of 10-35 GHz, and a phase noise floor as low as −132.16 dBc/Hz at 10 kHz is obtained. Compared to the PolM-based schemes, the use of a Dpol-MZM promises a cheaper cost and a potential for a higher measurement range up to 110 GHz [31]. The proposed scheme features compactness, high sensitivity and a wide measurement range, which can find applications in the evaluation of wideband tunable microwave signal sources.

REFERENCES

[1] *IEEE Standard Definitions of Physical Quantities for Fundamental Frequency and Time Metrology – Random Instabilities*, IEEE Standard 1139, 2008.

[2] A. K. Poddar, U. L. Rohde, and A. M. Apte, "How low can they go?: Oscillator phase noise model, theoretical, experimental validation, and phase noise measurements," *IEEE Microw. Mag.*, vol. 14, no. 6, pp. 50–72, Sep./Oct. 2013.

[3] U. L. Rohde, A. K. Poddar, and A. M. Apte, "Getting its measure: Oscillator phase noise measurement techniques and limitations," *IEEE Microw. Mag.*, vol. 14, no. 6, pp. 73–86, Sep./Oct. 2013.

[4] D. B. Leeson, "Oscillator phase noise: A 50-year review," *IEEE Trans. Ultrason. Ferroelect. Freq. Control*, vol. 63, no. 8, pp. 1208–1225, Aug. 2016.

[5] D. Eliyahu, D. Seidel, and L. Maleki, "Phase noise of a high performance OEO and an ultra low noise floor cross-correlation microwave photonic homodyne system," in *Proc. IEEE Int. Freq. Control Symp.*, Honolulu, HI, USA, 2008, pp. 811–814.

[6] X. Xie *et al.*, "Photonic microwave signals with zeptosecond-level absolute timing noise," *Nature Photon.*, vol. 11, no. 1, pp. 44–47, Nov. 2017.

[7] K. Siddiq, R. J. Watson, S. R. Pennock, P. Avery, R. Poulton, and B. Dakin-Norris, "Phase noise analysis in FMCW radar systems," in *Proc. Eur. Microw. Conf.*, Paris, France, 2015, pp. 1523–1526.

[8] A. G. Armada and M. Calvo, "Phase noise and sub-carrier spacing effects on the performance of an OFDM communication system," *IEEE Commun. Lett.*, vol. 2, no. 1, pp. 11–13, Jan. 1998.

[9] M. Nebel and B. Lankl, "Oscillator phase noise as a limiting factor in stand-alone GPS-indoor navigation," in *Proc. 5th ESA Workshop Satell. Navigation Technol. Eur. Workshop GNSS Signals Signal Process.*, Noordwijk, The Netherlands, 2010, pp. 1–8.

[10] E. Rubiola, E. Salik, S. Huang, N. Yu, and L. Maleki, "Photonic-delay technique for phase-noise measurement of microwave oscillators," *J. Opt. Soc. Amer. B*, vol. 22, no. 5, pp. 987–997, May 2005.

[11] Y. Xie, P. Zhou, Z. Jiang, Z. Zhou, Z. Song, and N. Li, "A compact photonic-delay line phase noise measurement system based on an electro-absorption modulated laser," in *Proc. Photon. Electromagn. Res. Symp.*, Hangzhou, China, 2021, pp. 801–804.

[12] N. Kuse and M. E. Fermann, "Electro-optic comb based real time ultra-high sensitivity phase noise measurement system for high frequency microwaves," *Sci. Rep.*, vol. 7, no. 1, pp. 2847, Jun. 2017.

[13] F. Zhang, J. Shi, Y. Zhang, D. Ben, L. Sun, and S. Pan, "Self-calibrating and high-sensitivity microwave phase noise analyzer applying an optical frequency comb generator and an optical-hybrid-based I/Q detector," *Opt. Lett.*, vol. 43, no. 20, pp. 5029–5032, Oct. 2018.

[14] X. Wang, X. S. Yao, P. Hao, T. Feng, X. Chen, and Y. Chong, "Ultra-low phase noise measurement of microwave sources using carrier suppression enabled by a photonic delay line," *J. Lightw. Technol.*, vol. 39, no. 22, pp. 7028–7039, Sep. 2021.

[15] J. Shi, F. Zhang, and S. Pan, "Phase noise measurement of RF signals by photonic time delay and digital phase demodulation," *IEEE Trans. Microw. Theory Techn.*, vol. 66, no. 9, pp. 4306–4315, Sep. 2018.

[16] F. Zhang, J. Shi, and S. Pan, "Wideband microwave phase noise measurement based on photonic-assisted I/Q mixing and digital phase demodulation," *Opt. Exp.*, vol. 25, no. 19, pp. 22 760–22 768, Sep. 2017.

[17] J. Shi, F. Zhang, D. Ben, and S. Pan, "Wideband microwave phase noise analyzer based on an all-optical microwave I/Q mixer," *J. Lightw. Technol.*, vol. 36, no. 19, pp. 4319–4325, Oct. 2018.

[18] Z. Jiang, P. Zhou, R. Zhang, K. Li, and N. Li, "Photonics-based dual-functional system for microwave signal generation and phase noise measurement," in *Proc. Asia Commun. Photon. Conf.*, Shanghai, China, 2021, Paper T3E.4.

[19] Z. Fan, Q. Qiu, J. Su, T. Zhang, and Y. Lin, "Phase noise measurement of an optoelectronic oscillator based on the photonic-delay line cross-correlation method," *Opt. Lett.*, vol. 44, no. 8, pp. 1992–1995, Apr. 2019.

[20] J. Shi, F. Zhang, D. Ben, and S. Pan, "Photonic-assisted single system for microwave frequency and phase noise measurement," *Chin. Opt. Lett.*, vol. 18, no. 9, Sep. 2020, Art. no. 092501.

[21] D. Zhu, F. Zhang, P. Zhou, D. Zhu, and S. Pan, "Wideband phase noise measurement using a multifunctional microwave photonic processor," *IEEE Photon. Technol. Lett.*, vol. 26, no. 24, pp. 2434–2437, Dec. 2014.

[22] W. Wang, J. Liu, H. Mei, W. Sun, and N. Zhu, "Photonic-assisted wideband phase noise analyzer based on optoelectronic hybrid units," *J. Lightw. Technol.*, vol. 34, no. 14, pp. 3425–3431, Jul. 2016.

[23] D. Zhu, F. Zhang, P. Zhou, and S. Pan, "Phase noise measurement of wideband microwave sources based on a microwave photonic frequency down-converter," *Opt. Lett.*, vol. 40, no. 7, pp. 1326–1329, Apr. 2015.

[24] F. Zhang, D. Zhu, and S. Pan, "Photonic-assisted wideband phase noise measurement of microwave signal sources," *Electron. Lett.*, vol. 51, no. 16, pp. 1272–1274, Aug. 2015.

[25] W. Wang *et al.*, "A wideband photonic microwave phase shifter using polarization-dependent intensity modulation," *Opt. Commun.*, vol. 356, pp. 522–525, Dec. 2015.

[26] W. Liu, W. Li, and J. Yao, "An ultra-wideband microwave photonic phase shifter with a full 360° phase tunable range," *IEEE Photon. Technol. Lett.*, vol. 25, no. 12, pp. 1107–1110, Jun. 2013.

[27] *Versawave 40 Gb/s 5.0 V Polarization Modulator (Data Sheet)*, Ottawa, Canada: Versawave Technologies, pp. 2.

[28] J. Hong, A. Liu, and J. Guo, "Study on low-phase-noise optoelectronic oscillator and high-sensitivity phase noise measurement system," *J. Opt. Soc. Amer. A*, vol. 30, no. 8, pp. 1557–1562, Aug. 2013.

[29] *R&S SMA100B RF and Microwave Signal Generator (Data Sheet) Version 06.00*, Munich, Germany: Rohde & Schwarz, 2022, pp. 22–29. [Online]. Available: https://scdn.rohde-schwarz.com/ur/pws/dl_downloads/dl_common_library/dl_brochures_and_datasheets/pdf_1/SMA100B_dat-sw_en_5215-1018-22_v0700.pdf

[30] *Ultra-Narrow Bandwidth-Variable Tunable Filter CVF-300CL/BVF-300CL (Data Sheet)*, Tokyo, Japan: Alnair Labs, vol. 1, pp. 1–2. [Online]. Available: http://www.alnair-labs.com/download/BVF-300.pdf

[31] M. Xu *et al.*, "Dual-polarization thin-film lithium niobate in-phase quadrature modulators for terabit-per-second transmission," *Optica*, vol. 9, no. 1, pp. 61–62, Jan. 2022.

[32] G. Qi, J. Yao, J. Seregelyi, S. Paquet, and J. C. Bélisle, "Effects of amplified spontaneous emission noise of optical amplifiers on the phase noise of optically generated electrical signals," in *Proc. Photon. Appl. Nonlinear Opt., Nanophotonics, Microw. Photon.*, Toronto, Canada, vol. 5971, 2005, Art. no. 59712D.

[33] E. Salik, N. Yu, L. Maleki, and E. Rubiola, "Dual photonic-delay line cross correlation method for phase noise measurement," in *Proc. IEEE Int. Freq. Control Symp. Expo.*, Montreal, QC, Canada, 2004, pp. 303–306.

[34] Z. Fan, Q. Qiu, J. Su, T. Zhang, and N. Yang, "Photonic-delay line cross correlation method based on DWDM for phase noise measurement," *IEEE Photon. J.*, vol. 10, no. 1, Feb. 2018, Art. no. 5500509.